Dynamic Inversion-Based Control Design for Multi-Phase Tandem Tilt-Wing Flight

Daniel Milz and Marc May and Gertjan Looye

The attractiveness of (tandem) tilt-wing electric vertical take-off and landing (eVTOL) vehicles has increased over the past decade due to their efficient wing-borne cruise flight and reduced requirements on ground-based infrastructure. However, this results in a complex flight control task, which must cover both the hover and cruise regimes, as well as the transition between them. In this regard, nonlinear dynamic inversion-based control approaches have been demonstrated to offer an effective solution. The intrinsic characteristics of these vehicles require that the controller operates across multiple flight phases, which differ in their dominant dynamics. This necessitates the implementation of multi-phase control strategies and a corresponding design approach. Dynamic inversion decouples the dynamics, providing a clean interface to the higher-level control functions. Furthermore, the controller is extended to utilize the pitch channel complementary to the tilt angle. The control system is evaluated on a six-degree-of-freedom flight dynamic model based on strip theory. The results demonstrate that the system is capable of performing a full transition. Additionally, pitch-supported tilting extends the flight envelope and accelerates the transition maneuver.

Milz, Daniel and May, Marc and Looye, Gertjan (2025) Dynamic Inversion-Based Control Design for Multi-Phase Tandem Tilt-Wing Flight. In: AIAA Scitech 2025 Forum, 2025. AIAA Scitech 2025 Forum, 6-10 Jan 2025, Orlando, FL. DOI: 10.2514/6.2025-2698

Dynamic Inversion-based Control Design for Multi-Phase Tandem Tilt-Wing Flight

Daniel Milz* and Marc May†
Institute of System Dynamics and Control, German Aerospace Center (DLR), 82234 Weßling, Germany
TUM School of Engineering and Design, Technical University of Munich (TUM), 85521 Ottobrunn, Germany

Gertjan Looye‡
Institute of System Dynamics and Control, German Aerospace Center (DLR), 82234 Weßling, Germany

The attractiveness of (tandem) tilt-wing electric vertical take-off and landing (eVTOL) vehicles has increased over the past decade due to their efficient wing-borne cruise flight and reduced requirements on ground-based infrastructure. However, this results in a complex flight control task, which must cover both the hover and cruise regimes, as well as the transition between them. In this regard, nonlinear dynamic inversion-based control approaches have been demonstrated to offer an effective solution. The intrinsic characteristics of these vehicles require that the controller operates across multiple flight phases, which differ in their dominant dynamics. This necessitates the implementation of multi-phase control strategies and a corresponding design approach. Dynamic inversion decouples the dynamics, providing a clean interface to the higher-level control functions. Furthermore, the controller is extended to utilize the pitch channel complementary to the tilt angle. The control system is evaluated on a six-degree-of-freedom flight dynamic model based on strip theory. The results demonstrate that the system is capable of performing a full transition. Additionally, pitch-supported tilting extends the flight envelope and accelerates the transition maneuver.

I. Introduction

Transformational vehicles are of particular interest due to their ability to take off and land independently of infrastructure while providing efficient wing-borne flight. Technologically, studying transformational vehicles is of great interest as they can perform maneuvers and missions that are otherwise impossible for conventional aircraft. While their primary applications will be in cargo delivery and advanced air mobility, they may also be interesting for combat, search and rescue operations, and rugged terrain and situations. It should also be noted that transformational eVTOLs are best suited to specific operational applications. Those requiring short-distance connections and operations requiring prolonged hover times are more effectively served by helicopters, multicopters, or trains and cars. Conversely, fixed-wing aircraft can more efficiently cover long-distance connections and connections with suitable infrastructure at the start and end points, including STOL configurations. Nevertheless, in their niche of infrastructure-agnostic, medium-distance, on-demand transportation, transformational eVTOLs possess a significant advantage.

In the category of transformational aircraft, tilt-rotors and tilt-wings are the most promising candidates [1]. However, in contrast to tilt-wings, tilt-rotor vehicles require complex propulsion systems and have drawbacks in aerodynamic efficiency [2]. Nevertheless, there are several reasons why tilt-wings have not been adopted to date. The main one is the technological challenge, which includes the battery technology but also the complex mechanics of the tilting mechanism and complex aerodynamics. Moreover, certification issues still need to be solved across most eVTOL categories. Furthermore, future eVTOL pilots face high requirements because transformational eVTOLs operate unprecedentedly, combining helicopter and aircraft modes. As a result, pilots have difficulties controlling these vehicles. An example is the three-hand problem of the Harrier jet, where the pilot must simultaneously operate the thrust lever, stick, and nozzle angle lever during take-off and landing [3], or the complex mechanical design of the CL-84, which ultimately led to crashes of the prototype [4]. Last but not least, public acceptance is a crucial point. Several important aspects that need to be met in order for consumers to use eVTOL transportation services have been identified [5]. The primary concerns

*Research Associate, Department of Aircraft Systems Dynamics, daniel.milz@dlr.de, AIAA member
†Research Associate, Department of Aircraft Systems Dynamics, marc.may@dlr.de
‡Head of Department, Department of Aircraft Systems Dynamics, gertjan.looye@dlr.de

are the safety implications of eVTOLs, given their novelty. These issues must be addressed to facilitate the market introduction of tilt-wing eVTOLs.

Our initial publication presented a proof-of-concept unified control law for tandem tilt-wing eVTOLs [6]. The work aimed to demonstrate the capability of dynamic inversion-based control approaches on tilt-wings. However, the flight dynamic model was simplified to include only the most significant effects. Over the subsequent years, our research focused on developing a more comprehensive flight dynamic model and retracing the various effects that influence the behavior of tandem tilt-wings [7]. Based on that, we proposed an optimization-based control allocation combined with dynamic inversion as a solution to the control task of the "high-fidelity" model of the tandem tilt-wing [8]. Finally, in [9], a sensory dynamic inversion-based controller for the attitude and the flight path of the tandem tilt-wing was developed while also a reduced model for the inversion, similar to [10], was introduced.

In contrast to similar approaches [11–14], this method simultaneously inverts the angular rate and velocity dynamics to generate thrust and tilt angle commands. The selection of controlled variables and the control structure is done *holistically* and non-switching, i.e., a *unified inversion*. It can be demonstrated that this approach is capable of controlling the tilt-wing [6, 9]. A similar holistic approach is done, e.g., in [15]. Nevertheless, at this point, no conclusions can yet be drawn regarding this approach's comparative advantages and disadvantages in relation to analogous research.

A. Problem Statement

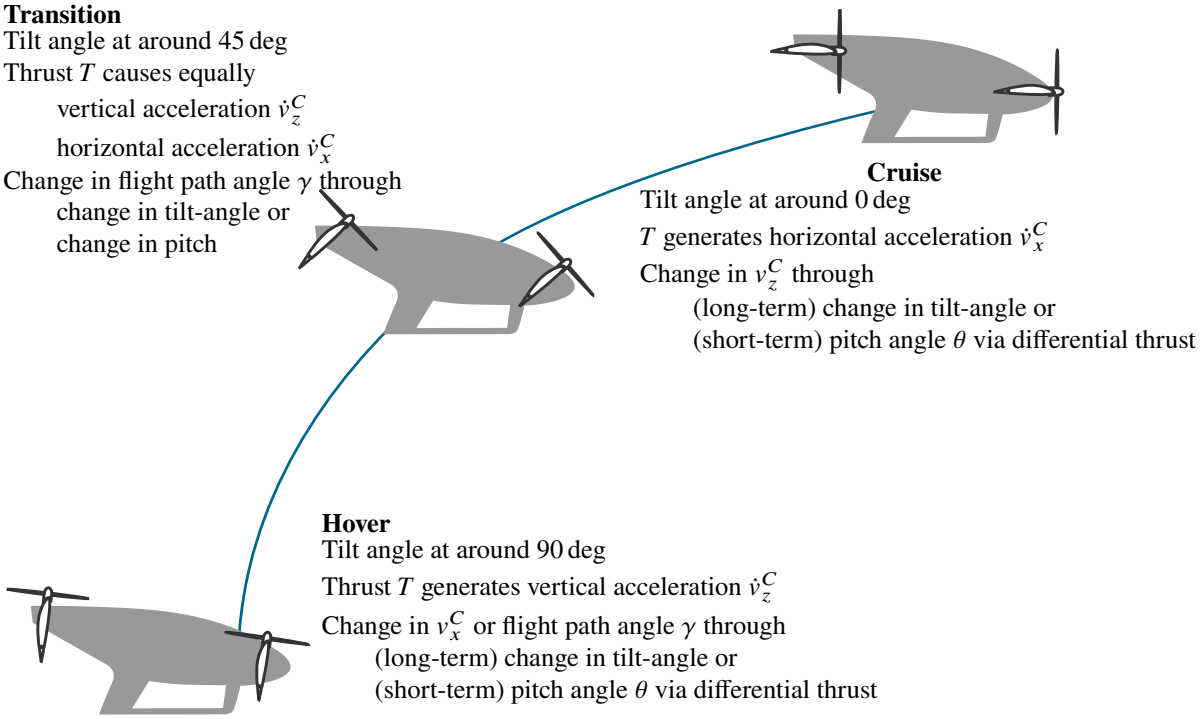

Fig. 1 Multi-phase flight with changing dynamics for the flight path control.

The issue of unified inversion of all axes is illustrated in Fig. 1. The inversion itself is not dependent on the dynamics of the actuator and effector; however, the control loops surrounding it are. The dynamics of the attitude and flight path control loops must be tuned to the dynamics of the plant. For most aircraft, these dynamics remain the same or are at least similar throughout the flight envelope. However, due to the nature of transformational vehicles, especially tandem tilt-wing eVTOLs, these dynamics change over the flight envelope, particularly for flight path control. For example, during hover, vertical acceleration is achieved by increasing thrust, whereas horizontal acceleration can be achieved by pitching forward or decreasing the wing tilt angle but vice versa during the cruise phase. These changes must be considered because the dynamics differ. While electric motors are typically characterized by a high bandwidth, tilt actuators are characterized by a low bandwidth. Consequently, the challenge arises in designing attitude and flight path controllers for the optimization-based control allocation within the sensory NDI, which can handle multiple flight

phases.

B. State-of-the-Art

New developments in transformational or tilt-wing eVTOL control include the application of dynamic inversion-based control methods to a (tandem) tilt-wing UAV [11–13, 16]. The control system is divided into a moment-controlling and force-controlling part to enable further uncoupling of motion. The moment-controlling part is expounded upon in [12]. It features an attitude controller, along with a (linear) control allocation strategy that can handle failures and integrates anti-wind-up techniques for saturating actuators. In [16], a universal method for outer-loop velocity control is presented. This approach simplifies the two-dimensional inversion problem (comprising vertical and horizontal velocity) into a one-dimensional problem by commanding a generalized force and tracking a compound velocity. The pitch attitude controller is utilized to stabilize and track the internal dynamics. While the approach is elegant and generic, the controller is tailored to track yaw rates and earth-centered velocities. Although this approach is favored for thrust-borne flight regimes, it is uncommon in wing-borne flight regimes.

Another current approach is applying learning-based control methods to a single tilt-wing UAV in order to be controlled [17]. Although the results show promising developments, the technology is still far from being applicable to certified environments. In [18], the authors show the development of a tool to tune controller parameters for eVTOLs.

The studies around [15] address the problem for a different eVTOL configuration, a lift+crusie vehicle, by adapting the inversion law and proposing a generic eVTOL control solution. They introduce virtual control variables, e.g., the roll and pitch angle, to ensure a well-working inversion. These variables are fed back to the controller input, offering an elegant solution. However, the approach does not directly support switching between commanded variables like the roll angle and lateral velocity without major blending efforts. Additionally, the tilt-wing aircraft's strong similarity between pitch and tilt angles (as shown later) cannot be employed directly by this approach.

C. Approach

The literature contains various approaches to the overall control problem of transformational VTOL aircraft, including tandem tilt-wing configurations, each with advantages and disadvantages. However, to our knowledge, no similar approach has been presented yet. The main objective is to develop a unified inversion approach that can be used to handle all vehicle-dependent characteristics, thereby allowing the independent implementation of outer-loop functions such as autoflight, piloted flight, and augmented/hybrid operations. This approach, however, entails a complex inversion problem. To overcome this challenge and to achieve a multi-phase flight (path) control design, these strategies have to be deployed:

1) Adjust the control variables to manage the multiple flight phases,
2) Adapt the controller structure to handle multi-phase flight,
    1a) Realize flight path changes by utilizing fast(er) pitch attitude control dynamics in the short term, followed by tilt-angle changes in the long term,
    1b) Implement a pilot control concept that allows handling the different flight phases smoothly,
3) Schedule control gains over the flight envelope to adapt to the changing dynamics,
4) Apply robust gain design methods to increase disturbance rejection and robustness to model uncertainties.

The third and fourth strategies are only briefly touched on and will be the subject of future research. The first strategy is an important step towards multi-phase flight. Our previous publications [8, 9] utilized the kinematic frame, a standard frame for fixed-wing flight path control, but this approach encounters issues during the hover. Specifically, the flight path and course angle become undefined when hovering with zero velocity, and the course angle jumps 180° when flying backward. The second strategy introduces a novel inner-loop design. The long-term changes, as illustrated in Fig. 1, represent the *optimal* or efficient solution. However, those are typically governed by slow dynamics. To enhance control performance and stabilize the aircraft effectively, we employ faster (though potentially less efficient or optimal) dynamics that fade into long-term changes. This strategy combines short-term, quick maneuvers with long-term, optimal ones to improve overall performance. Fig. 2 illustrates how utilizing the pitch motion can help increase the performance of the tilt-wing dynamics.

This is realized by a strategy similar to pseudo-control hedging (PCH) [19]. The basic idea is to use the excess of a virtual tilt angle command as a pitch angle command exhibiting faster dynamics. The virtual tilt command is the unrestricted tilt angle command and includes angles below the lower limit (0°) and above the upper limit (90°). Thus, it is possible to extend the flight envelope and enable (faster) backward and descending flights. However, this approach requires a well-tuned reference model to avoid constant hedging.

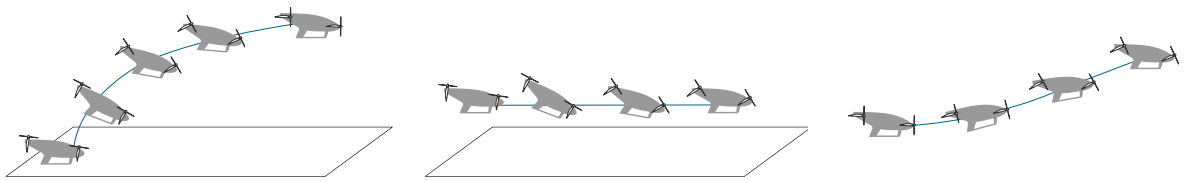

(a) Climbing transition maneuver **(b) Horizontal motion during hover** **(c) Vertical motion during cruise**

Fig. 2 Sketch of the pitch motion supporting the transition which is governed by slow tilt-wing dynamics.

Furthermore, in order to control all six degrees of freedom in the corresponding flight phase, a control concept is needed. While the proposed approach from [15] does not (inherently) require an adaptation of the control commands, this approach does need coordination and blending. Thus, an approach building on [6] is utilized. However, the implementation, tuning, and analysis of the control concept is part of future work.

II. Flight Dynamic Model

Let $x \in \mathrm{R}^{n_x}$ denote the state vector, $u \in \mathrm{R}^{n_u}$ the input vector, $y \in \mathrm{R}^{n_y}$ the output vector. Furthermore, let $f : \mathrm{R}^{n_x} \mapsto \mathrm{R}^{n_x}$, $g : \mathrm{R}^{n_x} \times \mathrm{R}^{n_u} \mapsto \mathrm{R}^{n_x}$, and $h : \mathrm{R}^{n_x} \mapsto \mathrm{R}^{n_y}$ be smooth vector fields representing the *internal*, *input*, and *output* dynamics, respectively. Then, a nonlinear, non-affine state-space system can be written as

$$\dot{x} = f(x) + g(x, u) \tag{1a}$$

$$\begin{bmatrix} y_{\text{com}} \\ y_{\text{add}} \end{bmatrix} = h(x) \tag{1b}$$

where the output is separated into the commanded part y_{com}, which will be the input of the inversion law, and additional sensor measurements y_{add}, which provide additional information and allow the reconstruction of the state vector. In this paper, we assume full-state observability and sufficient smoothness of $g(x, u)$ in u so that nonlinear equation solvers can be applied. This abstract state-space system forms the basis for the flight dynamic model and the control design.

Let the state vector be represented by $\boldsymbol{r}$ denoting the aircraft position in the earth frame, $\boldsymbol{\theta}$ the Euler angle attitude, $\boldsymbol{v}^B$ the aircraft velocity in body frame, $\boldsymbol{\omega}^B$ the angular rates in the body frame, and $\boldsymbol{\sigma}$ the transformational state. Furthermore, let $\mathbb{T}_{NB}$ and $\mathbb{T}_{\Phi B}$ denote the transformation matrix from the body frame to the earth frame and the direct cosine matrix of the Euler angles, respectively, $\boldsymbol{J}$ the moment of inertia, m the total mass, and $\boldsymbol{f}^B$ and $\boldsymbol{m}^B$ the respective forces and moments in body frame. Then, the nonlinear state space representation of the tandem tilt-wing eVTOL can be described by

$$\underbrace{\begin{bmatrix} \dot{\boldsymbol{r}} \\ \dot{\boldsymbol{\theta}} \\ \dot{\boldsymbol{v}}^B \\ \dot{\boldsymbol{\omega}}^B \\ \dot{\boldsymbol{\sigma}} \end{bmatrix}}_{\dot{x}} = \underbrace{\begin{bmatrix} \mathbb{T}_{NB}(\theta)\, \boldsymbol{v}^B \\ \mathbb{T}_{\Phi B}(\theta)\, \boldsymbol{\omega}^B \\ \frac{1}{m}\boldsymbol{f}_x^B(x) - \boldsymbol{\omega}^B \times \boldsymbol{v}^B \\ \boldsymbol{J}^{-1}\left(\boldsymbol{m}_x^B(x) - \boldsymbol{\omega} \times \boldsymbol{J}\boldsymbol{\omega}\right) \\ f_\sigma(x) \end{bmatrix}}_{f(x)} + \underbrace{\begin{bmatrix} 0 \\ 0 \\ \frac{1}{m}\boldsymbol{f}_u^B(x, \boldsymbol{u}) \\ \boldsymbol{J}^{-1}\boldsymbol{m}_u^B(x, \boldsymbol{u}) \\ g_\sigma(x, u) \end{bmatrix}}_{g(x,u)} \tag{2}$$

where $\boldsymbol{f}_x$, $\boldsymbol{f}_u$, $\boldsymbol{m}_x$, and $\boldsymbol{m}_u$ are the forces and moments, produced either the states or a combination of states and inputs. Fig. 3 shows a sketch of the tandem tilt-wing model with inputs annotated, i.e., the elevons $\delta_{\text{e},i}$, the tilt-wing angles $\delta_{\text{w},i}$, and the propeller thrusts T_i. The aerodynamic forces and moments are calculated by a semi-empirical strip-theory model, which is available in multiple versions with varying levels of fidelity. A high-fidelity version of the model, described in [7], serves as a reference and validation, while several reduced models, such as those presented in [8, 10], are used for simulation, control design, and analysis. This study's flight dynamic model is based on a three-strip-per-half-wing configuration, which considers propeller effects, as detailed in [9]. However, for the inversion, a more simplified model is employed, consisting of only two strips per half-wing, each located behind a propeller, and considering only the axial component of the propeller slipstream.

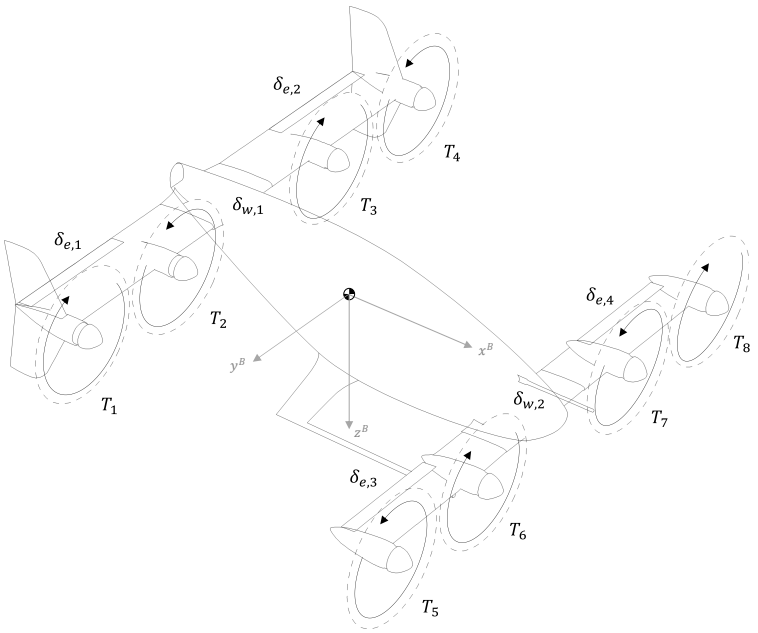

Fig. 3 3D view of the tandem tilt-wing configuration.

A. Reduced Longitudinal Model

In order to arrive at a simpler model for flight control design and understand the prevailing effects, the dynamics are reduced to a longitudinal model. This has the advantage that all strips on one wing can be combined into a single strip, resulting in only two strips, one for the front wing and one for the rear wing. Although this drastically reduces the complexity and presents an analytically manageable model, [20] suggests that even reducing the model to a single tilt-wing leads to comparable results. Furthermore, the equations are resolved in the control frame to get more insights and show the relation between pitch angle and tilt angle with

$$\begin{bmatrix} v_x^C \\ v_z^C \end{bmatrix} = \begin{bmatrix} \cos\theta & \sin\theta \\ -\sin\theta & \cos\theta \end{bmatrix} \begin{bmatrix} v_x^B \\ v_z^B \end{bmatrix} \tag{3}$$

The longitudinal model is characterized by the state variables, which are the pitch angle θ and the horizontal and vertical velocities, either v_x^B and v_z^B in the body frame or v_x^C and v_z^C in the control frame. Furthermore, ω^B denotes the angular rates in the body frame, C_D, C_L, and C_m denote the aerodynamic coefficients for the drag, lift, and pitch moment, α the angle of attack, δ_w the tilt angle, T the propeller thrust, m the total mass, S the reference wing area, $\bar{c}$ the reference chord length, and ρ the air density. The reduced longitudinal model can be stated as follows:

$$\begin{bmatrix} \dot{v}_x^B \\ \dot{v}_z^B \end{bmatrix} = g \begin{bmatrix} -\sin\theta \\ \cos\theta \end{bmatrix} + \begin{bmatrix} -\omega_y^B v_z^B \\ \omega_y^B v_x^B \end{bmatrix} + \frac{1}{m} f_u(v^B, \delta, T) \tag{4a}$$

$$\dot{\theta} = \omega_y^B = \frac{1}{2}\rho V^W(v^B, \delta, T)^2 \, S \frac{\bar{c}}{\omega_y^B} C_m(\alpha^W) + m_u^B \tag{4b}$$

with the generalized input moment m_u^B used as an input and the input force f_u^B:

$$f_u^B(v^B, \delta, T) = T \begin{bmatrix} \cos\delta \\ -\sin\delta \end{bmatrix} - \frac{1}{2}\rho \, V^W(v^B, \delta, T)^2 \, S \begin{bmatrix} \cos\left(\alpha^W - \delta\right) & -\sin\left(\alpha^W - \delta\right) \\ \sin\left(\alpha^W - \delta\right) & \cos\left(\alpha^W - \delta\right) \end{bmatrix} \begin{bmatrix} C_D(\alpha^W(v^B, \delta, T)) \\ C_L(\alpha^W(v^B, \delta, T)) \end{bmatrix}$$

The velocities in wing frame can be described using the slipstream-induced velocity v_i^W as

$$V^W(v^B, \delta, T) = \sqrt{v_x^W(T, \delta, v^B)^2 + v_z^W(\delta, v^B)^2} \tag{5a}$$

$$v_{x,s}^W(v^B, \delta, T) = \cos\delta v_x^B - \sin\delta v_z^B + v_i^W(v^B, \delta, T) \tag{5b}$$

$$v_z^W(v^B, \delta) = \cos\delta v_z^B + \sin\delta v_x^B \tag{5c}$$

$$v_i^W(v^B, \delta, T) = s_{sc}\left(-\frac{\cos\delta v_x^B - \sin\delta v_z^B}{2} + \frac{1}{2}\sqrt{\left(\cos\delta v_x^B - \sin\delta v_z^B\right)^2 + \frac{2T}{\rho\pi R^2}}\right) \tag{5d}$$

and the effective angle of attack as

$$\alpha^W(T, \delta, v^B) = \arctan\frac{v_z^W}{v_{x,s}^W} = \arctan\frac{\cos\delta v_z^B + \sin\delta v_x^B}{\cos\delta v_x^B - \sin\delta v_z^B + v_i^W(v^B, \delta, T)} = \arctan\left(\tan\left(\alpha^B + \delta\right)\frac{v_x^W}{v_{x,s}^W}\right) \tag{6}$$

by neglecting swirl effects and considering a propeller of radius R with a slipstream contraction factor s_{sc}.

As suggested in [15], using the control frame C can be an advantage for eVTOL control. It allows an intuitive control of the velocities and the flight path. Rewriting the single tilt-wing system into the control frame leads to the following dynamics:

$$\begin{bmatrix}\dot{v}_x^C\\ \dot{v}_z^C\end{bmatrix} = \begin{bmatrix}0\\ g\end{bmatrix} + \frac{T}{m}\begin{bmatrix}\cos(\theta+\delta)\\ -\sin(\theta+\delta)\end{bmatrix} - \frac{D(v^B, \delta, T)}{m}\begin{bmatrix}\cos\left(\theta+\delta-\alpha^W\right)\\ -\sin\left(\theta+\delta-\alpha^W\right)\end{bmatrix} - \frac{L(v^B, \delta, T)}{m}\begin{bmatrix}\sin\left(\theta+\delta-\alpha^W\right)\\ \cos\left(\theta+\delta-\alpha^W\right)\end{bmatrix} \tag{4a'}$$

with the velocities in the wing frame depending on v^C as

$$v_{x,s}^W(v^C, \delta+\theta, T) = \cos(\delta+\theta)\, v_x^C - \sin(\delta+\theta)\, v_z^C + v_i^W(v^C, \delta+\theta, T) \tag{5b'}$$

$$v_z^W(v^C, \delta+\theta) = \cos(\delta+\theta)\, v_z^C + \sin(\delta+\theta)\, v_x^C \tag{5c'}$$

$$v_i^W(v^C, \delta+\theta, T) = s_{sc}\left(-\frac{\cos(\delta+\theta)\, v_x^C - \sin(\delta+\theta)\, v_z^C}{2} + \frac{1}{2}\sqrt{\left(\cos(\delta+\theta)\, v_x^C - \sin(\delta+\theta)\, v_z^C\right)^2 + \frac{2T}{\rho\pi R^2}}\right) \tag{5d'}$$

and the reformulated effective angle of attacks, using the identity $\alpha^B = \alpha^C + \theta$, as

$$\alpha^W(T, \delta+\theta, v^C) = \arctan\left(\tan\left(\alpha^C + \theta + \delta\right)\frac{v_x^W}{v_{x,s}^W}\right) \tag{6'}$$

This shows that, simplified speaking, the tilt angle δ and pitch angle θ are alike.

III. Control Design

The basic control design for the tandem tilt-wing eVTOL was motivated and drafted in [6] and detailed in [8, 9] and is illustrated in Fig. 4. This approach employs a sensory nonlinear dynamic inversion control law combined with an optimization-based control allocation, which inverts the rotational and translational dynamics in one. In contrast, most previous works have employed a control concept with separated rotational inversion and translational control [12, 13, 21, 22]. However, combining both makes it possible to leverage specific vehicle characteristics and gain a more performant control solution. On the downside, this approach drastically increases the complexity of the inversion. However, if this block can be managed, all control functions built upon it can be realized relatively independently of the vehicle structure. This allows for a modular control design, in which individual control functions can be developed and integrated easily into the overall system. While the controller structure and the control allocation are similar to [9], this work uses a simplified model for the inversion, resolves the flight path or velocity controller in the control frame, adapts the attitude and velocity controller gains, and introduces pitch-supported tilting.

A. Sensory and Incremental Nonlinear Dynamic Inversion

Nonlinear Dynamic Inversion (NDI) [23] inverts the plant dynamics to get the input u_{NDI} necessary to achieve a given virtual control input $\nu = \dot{y}_{\mathrm{com}}$ by using an estimation of the state space function, $\hat{f}$ and $\hat{g}$, i.e., the on-board plant

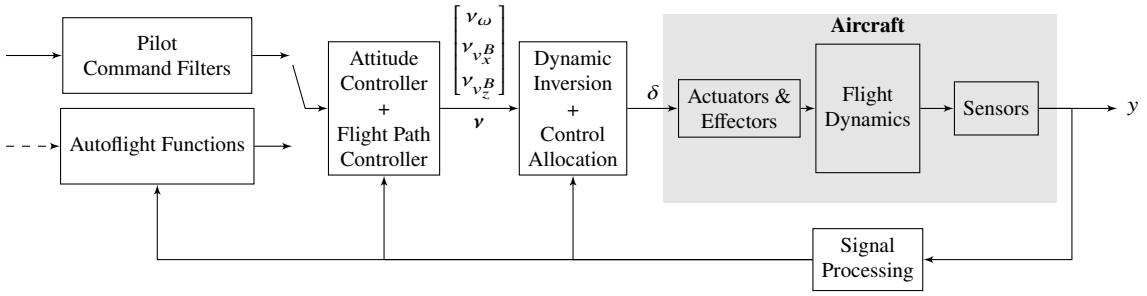

Fig. 4 Control architecture for dynamic inversion-based tandem tilt-wing control.

model. If $\dim u > \dim \nu$, then control allocation methods are required to solve the inversion problem [8]. Ganging is the most basic approach, e.g., combined differential deflection of ailerons or identical deflection of elevators. For now we assume that $\dim u = \dim \nu$. Then, the NDI control law can be written as

$$\hat{g}\left(\hat{x}, u_{\text{NDI}}\right) = \nu - \hat{f}(\hat{x}) \implies u_{\text{NDI}} = \hat{g}^{-1}\left(\hat{x},\, \nu - \hat{f}(\hat{x})\right) \tag{9}$$

with estimated state vector $\hat{x}$ and the inverse function $\hat{g}(\hat{x}, \hat{g}^{-1}(\hat{x}, z)) = z$ for a bijective function $\hat{g}$.

Sensory NDI approximates the estimated dynamics $\hat{f}(\hat{x})$ in (9) by sensor measurements of the state derivatives $\hat{\dot{x}}$ and inputs $\hat{u}$ as

$$\hat{f}(\hat{x}) \approx \hat{\dot{x}} - \hat{g}(\hat{x},\, \hat{u}) \tag{10}$$

By using this approximation, the NDI law becomes the sensory NDI law, i.e.,

$$\hat{g}\left(\hat{x},\, u_{\text{sNDI}}\right) = \nu - \hat{\dot{x}} + \hat{g}(\hat{x},\, \hat{u}) \tag{11}$$

which can be solved in multiple ways [9]. The control law is equal to the incremental NDI law for $\hat{g}(\hat{x}, u) \approx \hat{G}(\hat{x})u$ if $\hat{G}(\hat{x})$ is invertible, but allows for an absolute control command. Using an incremental approach, i.e., linearizing around the current state and input measurements by using the 1st Taylor polynomial and ignoring higher-order terms, is also a common way to solve (11) and effectively leads to the incremental NDI control law

$$\hat{g}\left(\hat{x},\, u\right) \approx \hat{g}\left(\hat{x}, \hat{u}\right) + \left.\frac{\partial \hat{g}(x,u)}{\partial u}\right|_{\substack{x=\hat{x}\\u=\hat{u}}} (u - \hat{u}) \tag{12}$$

$$u \approx \left(\left.\frac{\partial \hat{g}(x,u)}{\partial u}\right|_{\substack{x=\hat{x}\\u=\hat{u}}}\right)^{-1} \left(\nu - \hat{\dot{x}}\right) + \hat{u} \tag{13}$$

In summary, the basic idea of sensory as well as incremental NDI is to replace the dependence on $\hat{f}$ with measurements of the state vector derivatives $\hat{\dot{x}}$ and the current input $\hat{u}$, according to (10), to achieve an inversion of the form (11) or (13). While both do not depend on $\hat{f}$, they are exposed to the measurements $\hat{\dot{x}}$ and $\hat{u}$, which need to be synchronized. Furthermore, both measurements have a direct link on the commanded control surface deflection u_{iNDI} or u_{sNDI}. These issues are well known [24–27]. However, the incremental nature of (13) requires control allocation algorithms to be applied on incremental inputs Δu instead of absolute inputs u.

B. Optimization-based Control Allocation with Dynamic Inversion Constraint

This lies the basis for sensory NDI control design. As indicated by the function $g(x, u)$ in (2), we will invert the dynamics of $\boldsymbol{\omega}^B$ and the x- and z-component $\boldsymbol{v}^B$ since we cannot control a force in y-direction directly. Essentially, we get the following control law for the tandem tilt-wing

$$\mathcal{G}(\hat{x}, u) = \begin{bmatrix} \boldsymbol{f}^B_{\text{u,x}}(\hat{x}, u) \\ \boldsymbol{f}^B_{\text{u,z}}(\hat{x}, u) \\ \boldsymbol{m}^B_{\text{u}}(\hat{x}, u) \end{bmatrix} = \begin{bmatrix} m \cdot \left(\nu_{v_x} - \hat{\boldsymbol{v}}_{\text{x}}\right) + \boldsymbol{f}^B_{\text{u,x}}(\hat{x}, \hat{u}) \\ m \cdot \left(\nu_{v_z} - \hat{\boldsymbol{v}}_{\text{z}}\right) + \boldsymbol{f}^B_{\text{u,z}}(\hat{x}, \hat{u}) \\ \boldsymbol{J} \cdot \left(\nu_{\omega} - \hat{\boldsymbol{\omega}}\right) + \boldsymbol{m}^B_{\text{u}}(\hat{x}, \hat{u}) \end{bmatrix} = \underbrace{\begin{bmatrix} m & & \\ & m & \\ & & \boldsymbol{J} \end{bmatrix} \begin{bmatrix} \nu_{v_x} - \hat{\boldsymbol{v}}_{\text{x}} \\ \nu_{v_z} - \hat{\boldsymbol{v}}_{\text{z}} \\ \nu_{\omega} - \hat{\boldsymbol{\omega}} \end{bmatrix}}_{\tau_0} + \mathcal{G}(\hat{x}, \hat{u}) \tag{14}$$

The issue with this formulation is that the control command u is defined implicitly. The inverse function theorem gives us a statement about the solvability of $\mathcal{G}$ in a neighborhood of a given u_0. In fact, the solvability is ensured if $\nabla_u \mathcal{G}(x,u)|_{\substack{x=\hat{x}\\u=u_0}}$ is invertible. A detailed discussion about the design of an optimization-based control allocation in combination with dynamic inversion for transformational eVTOLS is given in [8, 12] and for other configurations in [28, 29]. Subsequently, a brief introduction is given.

For the tandem tilt-wing configuration, control allocation is required in order to solve dynamic inversion problem. Therefore, a convex minimization objective is introduced, yielding

$$\min_{u\in\mathcal{U}} L(\hat{x},u) \quad \text{s.t. } \mathcal{G}(\hat{x},u) = \tau_0 \tag{15}$$

for an arbitraty scalar const function $L(x,u)$. In order to arrive at an explicit solution to the above problem, we utilize the Taylor series expansion in u to the second order for $L(x,u)$ and first order for $\mathcal{G}(x,u)$. Assuming sufficiently small residuals, we arrive at the surrogate problem of (15)

$$\min_{u\in\mathcal{U}} \nabla_u L(\hat{x},u_0)\,(u-u_0) + \frac{1}{2}\,(u-u_0)^T\,\nabla_{uu} L(\hat{x},u_0)\,(u-u_0) \tag{16a}$$

$$\text{s.t. } \underbrace{\nabla_u \mathcal{G}(\hat{x},u_0)}_{B}\,u = \underbrace{\tau_0 - \mathcal{G}(\hat{x},u_0) + \nabla_u \mathcal{G}(\hat{x},u_0)u_0}_{\tau} \tag{16b}$$

which can explicitly be solved as stated in [8] as

$$u = B^+\tau + \left(I - B^+B\right)\left(u_0 - \nabla_{uu} L(\hat{x},u_0)^{-1}\,\nabla_u L(\hat{x},u_0)\right) \tag{17}$$

with the pseudo-inverse $B^+ = \nabla_{uu} L(\hat{x},u_0)^{-1} B^T\left(B\,\nabla_{uu} L(\hat{x},u_0)^{-1}\,B^T\right)$.

C. Attitude Control

The attitude controller tracks the euler angle attitude $\boldsymbol{\theta}$ via the body angular accelerations $\dot{\boldsymbol{\omega}}^B$. Therefore, a kinematic inversion from euler angle accelerations into body angular accelerations is required (see Appendix A.A). The angular accelerations are tracked through the dynamic inversion with the virtual control inputs $\nu_\omega = \begin{bmatrix}\nu_p,\ \nu_q,\ \nu_r\end{bmatrix}^T$. The roll and pitch acceleration in body frame are calculated from ν_ϕ and ν_θ. Those are derived from the control law

$$\begin{bmatrix}\nu_\phi\\ \nu_\theta\end{bmatrix} = \left(K_\mathrm{p} + \frac{K_\mathrm{i}}{s}\right)\left(\begin{bmatrix}\phi_\mathrm{d}\\ \theta_\mathrm{d}\end{bmatrix} - \begin{bmatrix}\hat{\phi}\\ \hat{\theta}\end{bmatrix}\right) + K_\mathrm{d}\left(\begin{bmatrix}\dot{\phi}_\mathrm{d}\\ \dot{\theta}_\mathrm{d}\end{bmatrix} - \begin{bmatrix}\hat{\dot{\phi}}\\ \hat{\dot{\theta}}\end{bmatrix}\right) + K_\mathrm{ff}\begin{bmatrix}\ddot{\phi}_\mathrm{d}\\ \ddot{\theta}_\mathrm{d}\end{bmatrix} \tag{18}$$

$$\nu_\mathrm{r} = \left(K_\mathrm{p} + \frac{K_\mathrm{i}}{s}\right)(r_\mathrm{d} - \hat{r}) \tag{19}$$

with controller gains K. The desired roll and pitch angles and derivatives are calculated through a second-order reference model. The attitude controller is equivalent to the one described in [6].

For the yaw axis either a tracking of $\dot{\psi}$ in hover or n_y in cruise flight is performed. The lateral load factor n_y is controlled through the sideslip angle β by using the approximations $r \approx \dot{\beta}$ and

$$\Delta n_y \approx \frac{1}{g}\,\bar{q}\,S\,C_{\mathrm{Y},\beta}\,\Delta\beta \tag{20}$$

When commanding a roll angle ϕ_com in cruise flight the aircraft performs a coordinated turn, i.e., $n_y = 0$. This can either be achieved solely by the previously mentioned n_y-controller (and neglecting the $\dot{\psi}$ error) or by using a feedforward $\dot{\psi}$-command of the coordinated turn and converting it to a feedforward r-command. This is done in accordance to the following formulas

$$\dot{\psi}_\mathrm{TC} \approx g\,\tan\phi\,\frac{v_x^C}{\left\|v^C\right\|_2} \tag{21a}$$

$$r_\mathrm{TC} \approx \dot{\psi}_\mathrm{TC}\,\cos\phi \tag{21b}$$

D. Flight Path Control

The flight path controller tracks the horizontal and vertical translational velocities in the control frame, v_x^C and v_z^C. The lateral velocity v_y^C is not controlled directly but via proxy commands in an outer loop by using translational rate command in hover mode and n_y control in cruise flight. The velocities are controlled by a PI controller

$$\begin{bmatrix} \nu_{v_x^C} \\ \nu_{v_x^C} \end{bmatrix} = \left(K_\mathrm{p} + \frac{K_\mathrm{i}}{s} \right) \left(\begin{bmatrix} v_{x,d}^C \\ v_{z,d}^C \end{bmatrix} - \begin{bmatrix} \hat{v}_x^C \\ \hat{v}_z^C \end{bmatrix} \right) + \begin{bmatrix} \dot{v}_{x,d}^C \\ \dot{v}_{z,d}^C \end{bmatrix} \tag{22}$$

For the inversion of the $\dot{v}^B$-equation, it is necessary to resolve the virtual control input in the body frame using a translational kinematic inversion (see Appendix A.B). The lateral virtual control input $\nu_{v_y^C}$ is thereby set to the measured value $\hat{v}_y^C$. The resulting virtual control input for the body velocities, ν_{v^B}, can be directly forwarded to the dynamic inversion. The gains in (22) depend on the longitudinal dynamics of the actuated plant and are heavily restricted by the bandwidth of the tilt actuator, as discussed and (partly) solved in Section III.E. An alternative approach is to schedule the gains based on the current transformation state σ.

E. Pitch-supported tilting

Examining equation (4a'), the similarity between the tilt angle δ and the pitch angle θ is evident. As illustrated in Fig. 2, pitch attitude control can enhance the performance of tilt-wing longitudinal flight path control. This can be achieved through a strategy similar to Pseudo Control Hedging (PCH) [19]: The control command u originates from the commanded pseudo control input ν but might exceed the dynamics' limits due to low effector bandwidths or actuator limits. Consequently, only a reduced pseudo-control $\hat{\nu}$ is achieved, resulting in a pseudo-control hedge $\nu_h = \nu - \hat{\nu}$, which is fed back to the reference model to hedge or inhibit the reference dynamics.

Tilt actuators have low bandwidths and thus restrict the dynamics of a tilt-wing aircraft. However, the pitch angle has a higher bandwidth and similar influence on the dynamics as the tilt angle, as shown in Section II.A. This motivates the use of the pitch angle to compensate for tilt angle error, which arises from its low bandwidth and deflection limits of 0° to 90°. These benefits can be leveraged by introducing the virtual tilt angle φ. The inversion law (15) calculates the optimal tilt angle for the current state and force (and moment) demand τ_0, which is limited to $-8T_\mathrm{max} \leq F_z^B \leq 0\,\mathrm{N}$ and $F_{x,\mathrm{min}}^B \leq F_x^B \leq 8T_\mathrm{max}$ as a precaution. The optimal tilt angle commands $\delta_{w,1..2}^*$ and thrust commands $T_{1..8}^*$ are calculated from τ_0. In contrast, the virtual tilt angle φ represents the direction of the ideal and unrestricted thrust vector that realizes the demanded forces in the x- and z-direction. To stay close to optimal command, the forces realized by the optimal commands summed with the τ_0-excess, i.e., the difference between the total demand τ_0 and the limited demand $\tau_{0,\mathrm{lim}}$, yield the virtual tilt angle:

$$\varphi = \arctan \frac{\sin \bar{\delta}_w^* \bar{T}^* - \tau_{0,z} + \tau_{0,\mathrm{lim},z}}{\cos \bar{\delta}_w^* \bar{T}^* + \tau_{0,x} - \tau_{0,\mathrm{lim},x}} \tag{23}$$

with the mean of the commanded tilt angles $\bar{\delta}_w^*$ and the mean of the commanded thrusts $\bar{T}^*$. The difference between this ideal tilt angle φ and the actual mean tilt angle $\bar{\hat{\delta}}_w = \frac{1}{2}\hat{\delta}_{w,1} + \frac{1}{2}\hat{\delta}_{w,2}$ is the new pitch angle command, i.e., $\theta_\mathrm{com} = \varphi - \bar{\hat{\delta}}_w$. The controller structure with pitch-supported tilting is depicted in Fig. 5.

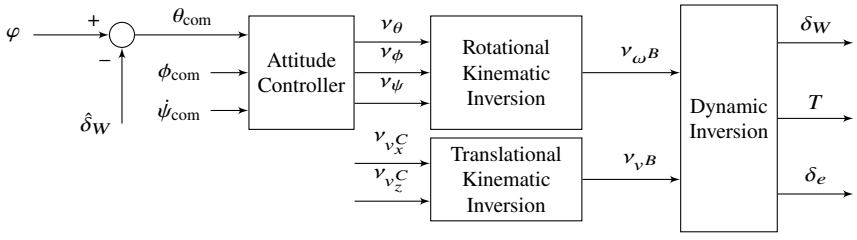

Fig. 5 Inner loop control structure with pitch-supported tilting.

IV. Simulation Results

The simulation setup is similar to [8, 9]. The flight dynamics model is described in detail in [30]. As the basic capabilities of the controller and the global inversion have already been investigated in [9], this work focuses solely on the benefits of the newly introduced concepts. Therefore, the first experiment covers a backward hover flight. The second experiment investigates the forward transition maneuver.

A. Backward flight

The first experiment investigates the capability of hovering backwards. The aircraft starts in a trimmed hover flight, i.e., $v^C = 0\,\frac{\mathrm{m}}{\mathrm{s}}$, $\dot{v}^C = 0\,\frac{\mathrm{m}}{\mathrm{s}^2}$, $\theta = 0°$, $\omega^B = 0\,\frac{°}{\mathrm{s}}$, and $\dot{\omega}^B = 0\,\frac{°}{\mathrm{s}^2}$. A step in velocity with a final value of $v_x^C = -5\,\frac{\mathrm{m}}{\mathrm{s}}$ is commanded after 5 s. Figure 6 shows the results of this experiment.

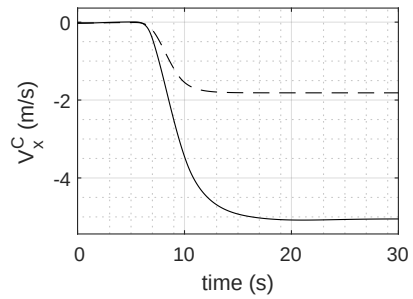

(a) Horizontal velocity v_x^C.

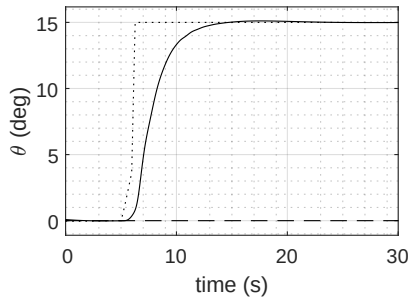

(b) Pitch angle θ with pitch command ·····.

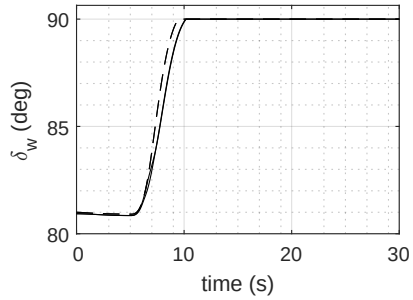

(c) Tilt angles $\delta_{w,1}$ and $\delta_{w,2}$.

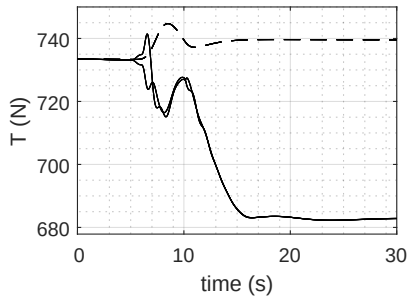

(d) Thrust settings $T_{1..8}$.

Fig. 6 Backward flight with a commanded velocity of $v_x^C = -5\,\frac{\mathrm{m}}{\mathrm{s}}$ with (——) and without (- - -) pitch-supported tilting.

Although backward flight is already possible without considering the pitch axis due to the slipstream-induced lift, the maximum backward velocity is at around $v_x^C = -1.8\,\frac{\mathrm{m}}{\mathrm{s}}$. When utilizing the pitch axis with a pitch angle limit of ±15°, it is possible to expand the envelope for the backward velocity to at least $v_x^C = -5\,\frac{\mathrm{m}}{\mathrm{s}}$ without causing problematic or unstable conditions.

B. Forward transition

The second experiment investigates the forward transition maneuver. In this scenario, the aircraft starts in a trimmed hover flight similar to the first experiment. A step in velocity at 5 s with a final value of $v_x^C = 40\,\frac{\mathrm{m}}{\mathrm{s}}$, i.e., cruise flight, while keeping the attitude constant. Figure 7 shows the results of this experiment.

Fig. 7a shows the forward velocity v_x^C during the transition maneuver for both cases. It can be seen, that by utilizing the pitch channel in addition to the tilt angle, it is possible to accelerate the transition maneuver by overcoming the slow bandwidth of the tilt actuator with the faster pitch dynamics. In order to get a quantitative characterization, the step response in analyzed. The step response in v_x^C is characterized by rise time t_r from 10 % to 90 % of 40 $\frac{\mathrm{m}}{\mathrm{s}}$, the settling time t_s for maximum deviation of 2.5 % of the peak error, the overshoot o, and the mean total thrust $\bar{T} = \frac{\Delta t}{t_{\mathrm{end}}} \sum_i T_i$ which are stated in Table 1.

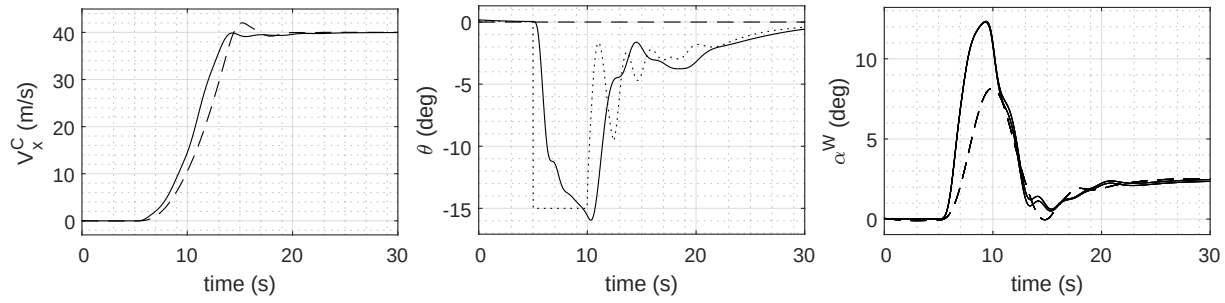

(a) Horizontal velocity v_x^C. **(b) Pitch angle θ with pitch command ⋯⋯.** **(c) Angle of attack α**

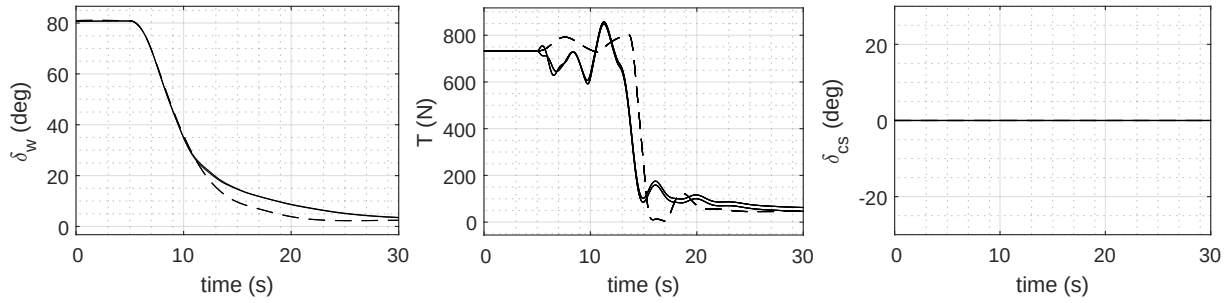

(d) Tilt angles $\delta_{w,1}$ and $\delta_{w,2}$. **(e) Thrust settings $T_{1..8}$.** **(f) Control surface deflection δ_e.**

Fig. 7 Forward transition with a commanded velocity of $v_x^C = 40\ \frac{\text{m}}{\text{s}}$ with (——) and without (- - -) pitch-supported tilting.

	Without pitch support	With pitch support
t_r	5.482 s	5.249 s
t_s	21.133 s	18.692 s
o	5.054 %	0 %
$\bar{T}$	4336 N	4187 N

Table 1 Step response characteristics of the forward transition experiment.

V. Discussion

The objective of this study is to extend the existing flight control law [9] to facilitate multi-phase tandem tilt-wing flight. The capability to operate in different flight regimes with distinctive dominant dynamics is a crucial element of transformational eVTOL control. In the case of a tandem tilt-wing aircraft, the flight phases include the hover phase, analogous to a multicopter, the cruise phase, similar to a fixed-wing aircraft, and the transitions between these two phases. This research focuses on adapting the control law to represent the eVTOL's velocities in the more generic control frame, thereby enabling more intuitive navigation and control. Furthermore, the concept of *pitch-supported tilting* is introduced, which leverages the pitch channel to augment the tilting motion, effectively broadening the flight envelope. Consequently, the effective tilt angle can be extended beyond the physical tilt angle limits, allowing for angles of greater than 90° and less than 0°. Additionally, this strategy accelerates transition maneuvers by combining the faster pitch angle dynamics with slower tilt angle dynamics, resulting in enhanced overall performance.

The experimental results presented in Section IV.A demonstrate the efficacy of both the control frame representation and pitch-supported tilting. The representation of commanded velocities in the control frame during hover enables intuitive navigation of the aircraft in any direction. Notably, commanding a negative velocity in the x-direction results in a backward hover flight. This maneuver is also enhanced through pitch-supported tilting. Although the slipstream effect engenders backward hover flight with a tilt angle of 90° while maintaining a pitch angle of 0°, the velocity is limited to $-1.8\ \frac{\text{m}}{\text{s}}$. By permitting pitch angles of up to 15°, a controlled backward flight with a velocity of at least $-5\ \frac{\text{m}}{\text{s}}$ can be attained.

The second experiment, presented in Section IV.B, investigates the forward transition of the vehicle starting in hover mode and commanding $v_x^C = 40\,\frac{\mathrm{m}}{\mathrm{s}}$, which corresponds approximately to the cruise speed. Transition maneuvers are critical for tilt-wing aircraft operation, as they can lead to high angles of attack, potentially resulting in post-stall flight. However, by exploiting the slipstream effect and executing the transition rapidly, the effective angle of attack α^W can be reduced. The results depicted in Fig. 7 demonstrate that the transition can be successfully completed with and without pitch support. However, utilizing the pitch channel yields an improvement in performance. Both qualitative (Figs. 7a and 7e) and quantitative (Table 1) analyses reveal that pitch support accelerates the transition maneuver and reduces the mean thrust, which corresponds to a lower energy consumption. Although the rise times are fairly similar, the settling time is approximately 2.5 s faster, and no overshoot occurs.

VI. Conclusion

This research builds upon previous publications and incorporates an updated flight dynamics model and a refined reduced-order model for inversion, which collectively enhance the accuracy and efficiency of the controller. By redefining the controlled variables to include velocities in the control frame, the proposed approach enables a more intuitive control design and facilitates seamless transitions between different flight regimes. The introduction of pitch-supported tilting expands the flight envelope, allowing for faster transition maneuvers and more efficient execution of flight tasks such as backward flight. The sensory nonlinear dynamic inversion control law complemented by an optimization-based control allocation has been demonstrated to effectively leverage these advancements. The results of this study lay the groundwork for achieving multi-phase tandem tilt-wing flight.

Future research will address the remaining challenges, including the development of a more sophisticated reference model and linear control design, as well as the introduction of an intuitive pilot control framework that seamlessly integrates all flight regimes.

A. Appendix

A. Rotational Kinematic Inversion

$$\dot{\omega}^B = \underbrace{\left(\frac{\mathrm{d}}{\mathrm{d}t}\begin{bmatrix}1 & 0 & -\sin\theta\\ 0 & \cos\phi & \sin\phi\cos\theta\\ 0 & -\sin\phi & \cos\phi\cos\theta\end{bmatrix}\right)}_{\begin{bmatrix}0 & 0 & -\cos\theta\,\dot{\theta}\\ 0 & -\sin\phi\,\dot{\phi} & \cos\phi\cos\theta\,\dot{\phi} - \sin\phi\sin\theta\,\dot{\theta}\\ 0 & -\cos\phi\,\dot{\phi} & -\sin\phi\cos\theta\,\dot{\phi} - \cos\phi\sin\theta\,\dot{\theta}\end{bmatrix}} \underbrace{\begin{bmatrix}\dot{\phi}\\ \dot{\theta}\\ \dot{\psi}\end{bmatrix}}_{\begin{bmatrix}1 & \sin\phi\tan\theta & \cos\phi\tan\theta\\ 0 & \cos\phi & -\sin\phi\\ 0 & \frac{\sin\phi}{\cos\theta} & \frac{\cos\phi}{\cos\theta}\end{bmatrix}\omega^B} + \begin{bmatrix}1 & 0 & -\sin\theta\\ 0 & \cos\phi & \sin\phi\cos\theta\\ 0 & -\sin\phi & \cos\phi\cos\theta\end{bmatrix}\begin{bmatrix}\ddot{\phi}\\ \ddot{\theta}\\ \ddot{\psi}\end{bmatrix} \tag{24}$$

B. Translational Kinematic Inversion

$$\dot{v}^B = \underbrace{\left(\frac{\mathrm{d}}{\mathrm{d}t}\begin{bmatrix}\cos\theta & 0 & -\sin\theta\\ \sin\phi\sin\theta & \cos\phi & \sin\phi\cos\theta\\ \cos\phi\sin\theta & -\sin\phi & \cos\phi\cos\theta\end{bmatrix}\right)}_{\begin{bmatrix}-\sin\theta\,\dot{\theta} & 0 & -\cos\theta\,\dot{\theta}\\ \cos\phi\sin\theta\,\dot{\phi} + \sin\phi\cos\theta\,\dot{\theta} & -\sin\phi\,\dot{\phi} & \cos\phi\cos\theta\,\dot{\phi} - \sin\phi\sin\theta\,\dot{\theta}\\ -\sin\phi\sin\theta\,\dot{\phi} + \cos\phi\cos\theta\,\dot{\theta} & -\cos\phi\,\dot{\phi} & -\sin\phi\cos\theta\,\dot{\phi} - \cos\phi\sin\theta\,\dot{\theta}\end{bmatrix}} v^C + \begin{bmatrix}\cos\theta & 0 & -\sin\theta\\ \sin\phi\sin\theta & \cos\phi & \sin\phi\cos\theta\\ \cos\phi\sin\theta & -\sin\phi & \cos\phi\cos\theta\end{bmatrix}\dot{v}^C \tag{25}$$

References

[1] Bacchini, A., and Cestino, E., "Electric VTOL Configurations Comparison," *Aerospace*, Vol. 6, No. 3, 2019. https://doi.org/10.3390/aerospace6030026.

[2] Chana, W. F., and Sullivan, T., "The Tilt Wing Configuration for High Speed VSTOL Aircraft," *ICAS 1994*, 1994.

[3] Lombaerts, T., Kaneshige, J., and Feary, M., "Control Concepts for Simplified Vehicle Operations of a Quadrotor eVTOL Vehicle," *AIAA Aviation 2020 Forum*, 2020.

[4] Sullivan, T., "The Canadair CL-84 tilt wing design," *Aircraft Design, Systems, and Operations Meeting*, 1993. https://doi.org/10.2514/6.1993-3939.

[5] Al Haddad, C., Chaniotakis, M., Straubinger, A., Plötner, K., and Antoniou, C., "Factors affecting the adoption and use of urban air mobility," *Transportation Research Part A Policy and Practice*, Vol. 132, 2020, pp. Pages 696–712. https://doi.org/10.1016/j.tra.2019.12.020.

[6] Milz, D., and Looye, G., "Tilt-Wing Control Design for a Unified Control Concept," *AIAA SCITECH 2022 Forum*, 2022. https://doi.org/10.2514/6.2022-1084.

[7] May, M. S., Milz, D., and Looye, G., "Semi-Empirical Aerodynamic Modeling Approach for Tandem Tilt-Wing eVTOL Control Design Applications," *AIAA SCITECH 2023 Forum*, 2023. https://doi.org/10.2514/6.2023-1529.

[8] Milz, D., May, M., and Looye, G., "Dynamic Inversion-Based Control Concept for Transformational Tilt-Wing eVTOLs," *AIAA SciTech 2024 Forum*, AIAA, 2024. https://doi.org/10.2514/6.2024-1290.

[9] Milz, D., May, M., and Looye, G., "Tandem Tilt-Wing Control Design based on Sensory Nonlinear Dynamic Inversion," *AIAA AVIATION 2024 Forum*, 2024. https://doi.org/10.2514/6.2024-4418.

[10] May, M., Milz, D., and Looye, G., "Transition Strategies for Tilt-Wing Aircraft," *AIAA SciTech 2024 Forum*, AIAA, 2024. https://doi.org/10.2514/6.2024-1289.

[11] Di Francesco, G., and Mattei, M., "Modeling and Incremental Nonlinear Dynamic Inversion Control of a Novel Unmanned Tiltrotor," *Journal of Aircraft*, Vol. 53, No. 1, 2016, pp. 73–86. https://doi.org/10.2514/1.C033183.

[12] Panish, L., Nicholls, C., and Bacic, M., "Nonlinear Dynamic Inversion Flight Control of a Tiltwing VTOL Aircraft," *AIAA SCITECH 2023 Forum*, American Institute of Aeronautics and Astronautics, 2023. https://doi.org/10.2514/6.2023-1910.

[13] Binz, F., Islam, T., and Moormann, D., "Attitude control of tiltwing aircraft using a wing-fixed coordinate system and incremental nonlinear dynamic inversion," *International Journal of Micro Air Vehicles*, Vol. 11, 2019, p. 1756829319861370. https://doi.org/10.1177/1756829319861370, URL https://doi.org/10.1177/1756829319861370.

[14] Lombaerts, T., Kaneshige, J., Schuet, S., Aponso, B. L., Shish, K. H., and Hardy, G., "Dynamic Inversion based Full Envelope Flight Control for an eVTOL Vehicle using a Unified Framework," *AIAA Scitech 2020 Forum*, 2020. https://doi.org/10.2514/6.2020-1619.

[15] Raab, S. A., Zhang, J., Bhardwaj, P., and Holzapfel, F., "Proposal of a Unified Control Strategy for Vertical Take-off and Landing Transition Aircraft Configurations," *2018 Applied Aerodynamics Conference*, American Institute of Aeronautics and Astronautics, 2018. https://doi.org/10.2514/6.2018-3478.

[16] Panish, L., and Bacic, M., "A Generalized Full-Envelope Outer-Loop Feedback Linearization Control Strategy for Transition VTOL Aircraft," *AIAA AVIATION 2023 Forum*, American Institute of Aeronautics and Astronautics, 2023. https://doi.org/10.2514/6.2023-4511.

[17] Axten, R. M., Khamvilai, T., and Johnson, E. N., "VTOL Freewing Design and Adaptive Controller Development," *AIAA SCITECH 2023 Forum*, 2023. https://doi.org/10.2514/6.2023-0401.

[18] Surmann, D., and Myschik, S., "Gain Design of an INDI-based Controller for a Conceptual eVTOL in a Nonlinear Simulation Environment," *AIAA SCITECH 2023 Forum*, 2023. https://doi.org/10.2514/6.2023-1250.

[19] Johnson, E. N., and Calise, A. J., "Pseudo-control hedging: A new method for adaptive control," *Advances in navigation guidance and control technology workshop*, Alabama, USA Alabama, USA, 2000, pp. 1–2.

[20] May, M. S., Milz, D., and Looye, G., "Towards the Determination of the Dynamic Transition Corridor for Tandem Tilt-Wing Aircraft," *AIAA AVIATION FORUM AND ASCEND 2024*, 2024. https://doi.org/10.2514/6.2024-4417.

[21] Hartmann, P., Meyer, C., and Moormann, D., "Unified Approach for Velocity Control and Flight State Transition of Unmanned Tiltwing Aircraft," *AIAA Guidance, Navigation, and Control Conference*, 2016. https://doi.org/10.2514/6.2016-2101.

[22] Öner, K. T., Çetinsoy, E., Sirimoğlu, E., Hançer, C., Ünel, M., Akşit, M. F., Gülez, K., and Kandemir, I., "Mathematical modeling and vertical flight control of a tilt-wing UAV," *Turkish Journal of Electrical Engineering & Computer Sciences*, Vol. 20, No. 1, 2012, pp. 149–157.

[23] Enns, D., Bugajski, D., Hendrick, R., and Stein, G., "Dynamic inversion: an evolving methodology for flight control design," *International Journal of Control*, Vol. 59, No. 1, 1994, pp. 71–91. https://doi.org/10.1080/00207179408923070.

[24] Kier, T. M., Müller, R., and Looye, G., "Analysis of Automatic Control Function Effects on Vertical Tail Plane Critical Load Conditions," *AIAA Scitech 2020 Forum*, American Institute of Aeronautics and Astronautics, 2020. https://doi.org/10.2514/6.2020-1621.

[25] Steffensen, R., Steinert, A., Mbikayi, Z., Raab, S., Angelov, J., and Holzapfel, F., "Filter and sensor delay synchronization in incremental flight control laws," *Aerospace Systems*, 2023. https://doi.org/10.1007/s42401-022-00186-2.

[26] Kumtepe, Y., Pollack, T., and Kampen, E.-J. V., "Flight Control Law Design using Hybrid Incremental Nonlinear Dynamic Inversion," *AIAA SCITECH 2022 Forum*, American Institute of Aeronautics and Astronautics, 2022. https://doi.org/10.2514/6.2022-1597.

[27] Milz, D., May, M. S., and Looye, G., "Flight Testing Air Data Sensor Failure Handling with Hybrid Nonlinear Dynamic Inversion," *Proceedings of the 2024 CEAS EuroGNC conference*, 2024.

[28] Pollack, T., and Kampen, E.-J. V., "Multi-objective Design and Performance Analysis of Incremental Control Allocation-based Flight Control Laws," *AIAA SCITECH 2023 Forum*, 2023. https://doi.org/10.2514/6.2023-1249.

[29] Pfeifele, O., and Fichter, W., "Energy Optimal Control Allocation for INDI Controlled Transition Aircraft," *AIAA Scitech 2021 Forum*, 2021. https://doi.org/10.2514/6.2021-1457.

[30] May, M., Milz, D., Armanini, S. F., and Looye, G., "Impace of Failure on the Tilt-Wing eVTOL Backward Transition," *AIAA SciTech 2025 Forum*, AIAA, 2025.